Brackish water desalination for agriculture: assessing the performance of inorganic fertilizer draw solutions.

Wafa Suwaileh[a], Daniel Johnson[a], Nidal Hilal[a,b] *

[a]*Centre for Water Advanced Technologies and Environmental Research (CWATER), College of Engineering, Swansea University, Swansea, SA1 8EN, UK*

[b]*NYUAD Water Research Center, New York University Abdu Dhabi, Abu Dhabi, United Arab Emirates*

Corresponding author.

Email address: n.hilal@swansea.ac.uk (Nidal Hilal)

Abstract

Fertilizer drawn forward osmosis (FDFO) is a cost-effective technology for brackish water desalination. The diluted fertilizer draw solution can be used to supply nutrients to crops instead of separating it from the desalinated water. This work evaluates the performance of the FDFO using four fertilizer draw solutions with various concentrations (1.0, 1.5, 2.0 mol/L) and a polyamide thin film composite (TFC) FO membrane for brackish water desalination. The results

revealed that KCl fertilizer draw solution achieved the highest water flux and adequate reverse salt flux as compared to other fertilizer draw solution. The mixture KCl + KNO_3 and KH_2PO_4 fertilizer draw solution generated the lowest water permeation and reverse salt flux. KH_2PO_4 draw solute promoted the growth of salt scaling which affected the membrane productivity in terms of water flux. The negatively charge of the membrane surface was responsible for precipitation of salt on the selective layer. This influenced the performance and resulted in low water permeation and minimum loss of nutrients in the fertilizer draw solution. The advantage of FDFO is in not needing a recovery step to reconcentrate the draw solution, instead using diluted draw solution as a supplement to irrigation water via fertigation.

Keywords

Brackish water desalination, fertilizer drawn forward osmosis system, thin film composite membrane, draw solution, scaling.

1. Introduction

Water scarcity is a global problem and a substantial challenge for this century [1]. There are limited resources of pure water and the agriculture industry is the main consumer of pure water. Therefore, alternative resources of freshwater are needed due to increasing water demands and decreasing water supplies. Forward osmosis (FO) desalination is a membrane-based process that is receiving much attention nowadays. The FO system utilizes osmotic pressure gradient between the draw solution (DS), and the feed solution (FS) to drive water

across a semipermeable membrane from a dilute feed solution to a concentrated draw solution while hindering the transport of most solutes [2]. FO was applied to many areas, such as seawater and brackish water (BW) [3] wastewater treatment [4], the food industry [5], microalgal cell separation from source water [6], and energy generation [7].

To date, little academic research has been conducted on BW desalination [7, 8] and there has been no pilot-scale assessment conducted by industry due to high operating costs. Furthermore, the FO system still encounters challenges of the unavailability of suitable membranes for the FO process. Most earlier works are limited to commercial FO membranes, most of which were fabricated for reverse osmosis (RO) process. The development of an ideal membrane is of concern to researchers throughout the world [9]. The most widely used commercial membranes are cellulose acetate (CA), cellulose triacetate (CTA) from Hydration Technology Innovations (HTI, Albany, OR) [10], but they suffer low water permeation [9], low selectivity, are prone to biological attack and chemical hydrolysis [11]. Some great efforts have been focused on the development of a high-performance FO membrane over the last two decades [12, 13]; however, they are fabricated using lab scale techniques.

Additionally, several technological challenges such as internal concentration polarization (ICP), external concentration polarization (ECP), fouling, reverse solute flux have yet to be mitigated [14]. ICP is caused due to the diffusion of the concentrated draw solutes within the support layer which decreases the ultimate driving force across the membrane and reduction in the water permeation [15]. This effect has been observed when thin film composite (TFC) FO membrane was used for FO system due to the high porosity of the support layer. One of the main problems in FO operation is membrane scaling and fouling. Although some studies

have revealed that the FO system has a low tendency to fouling, other researchers have highlighted that the FO process is still influenced by severe fouling under some circumstances [15, 16]. Xie et al examined long term scaling on both CTA and TFC membranes and it was quantified in water flux reduction and scaling surface morphology [17]. One of the findings is that the surface chemistry of the membrane can induce scaling formation on the membrane. Therefore, TFC membrane is more susceptible to salt scaling than CTA membrane due to the interaction between carboxylic functional groups in the selective layer and salt components. To overcome these issues, an understanding of the properties of the support layer and the selective layer of ready-made membranes is necessary. Besides, the effect of these properties on the membrane productivity is crucial.

Another key factor that has hindered the successful development of the FO system is the availability of an ideal DS. Researchers have explored the possible effects of DS characteristics and mass transport resistance on the membrane performance. Fertilizer draw solutions are good candidates for the FO process and they were used in earlier studies [18]. Many inorganic fertilizer draw solutions have been investigated in the FO process and the diluted DS could be used for direct fertigation. The concept of fertigation refers to the use of a diluted fertilizer as an irrigation system to supply agricultural lands. One of its advantages is as a cost-effective method to provide required nutrients to plants and crops [18]. Inorganic fertilizers can be proposed to extract pure water from saline solutions and brackish water. The purpose is to reduce the cost of the brackish water desalination and removing the recovery system of the draw solution. Recovery of draw solutes and reconcentration is a major stumbling block to commercialization of FO process due to the energy costs involved. As such, much of the effort

in development of draw solutes is aimed at solutes with cheap recovery routes, or ones which do not need a recovery step at all [19]. After the FO filtration, the final diluted fertilizer DS becomes less concentrated and could be used for direct irrigation. However, a source of pure water must be available to further dilute the DS to adjust its concentration for irrigation on the field [20]. Despite the advantages of fertilizer draw solutions, when the DS components interact with a polymeric membrane, it may alter the membrane structure [21]. Furthermore, draw solute back diffusion not only accelerates the salt accumulation in the feed solution, but it may also increase the costs for replenishment of the lost draw solutes. When increasing the DS concentration, specific weight and density can be increased. These properties can reduce the solution mobility; thus, high energy consumption and pumping costs are required [18, 22]. All the above limitations may result in high operation and capital costs. Also, there are many unanswered questions on the effect of the above factors on the FO membrane performance.

In this work, the combinations of fertilizer compounds as draw solutions were used in conjunction with a polyamide (PA)-TFC membrane commercially manufactured (Toray Industries Inc.) specifically for FO processes as a potential method for improving the water permeability and reducing the reverse solute flux. However, the experimental results showed that the effect of this addition was a minimization for the reverse solute flux (RSF) associated with lower water permeation. Moreover, the effect of polyamide (PA)-TFC material on the water flux and reverse solute flux (RSF) was investigated as a potential commercially available membrane for FDFO process. Additionally, the composition and salinity concentration of the brackish

water (BW) feed was examined to highlight its effect on the membrane and fertilizer draw solutions performance.

1. Experimental

1.1 Membrane material and chemicals

1.1.1 Commercial FO membranes

TFC forward osmosis membrane coupons were utilized for all FDFO tests. CSM sheet membranes were supplied by Toray Chemical Korea Inc., Korea. These membranes have an asymmetric structure that is composed of three layers: 1-polyamide coating as a selective layer on the top, 2- an intermediate polysulfone porous substrate, and 3- a polyester support mesh embedded in the polysulfone substrate providing mechanical strength.

1.1.2 Draw solution

Fertilizer DSs used in this study were KCl, KNO_3, KH_2PO_4, and KCl+KNO_3, with NaCl also used for comparison. All chemicals were supplied as pure reagent grade from Merck, UK. These solutions were prepared by adding the solute to deionized water (DI) and pH adjusted to 3.5 to avoid increasing the pH of the feed solution. The total concentration of the DS was fixed at 1.0, 1.5 and 2.0 mol/L. Thermodynamic characteristics, such as osmotic pressure, viscosity, density, and speciation of the solutions, were predicted by using the OLI Stream

Analyzer 3.2. software (OLI Systems Inc., US), using a thermodynamic synthesized based on previous experimental data to measure the solution properties over many concentrations and temperatures [23].

1.1.2 Feed solutions

The FS was composed of synthesized synthesizedbrackish water. The composition of brackish water was taken from [24]. Synthesized brackish solutions were prepared with various total dissolved salts (TDSs) of 5,000 - 10,000 - 15,000 and 20,000 mg/L or parts per million (ppm) by adding NaCl, $MgCl_2$, Na_2SO_4, KCl, and $CaCl_2$ to DI water. All chemicals were reagent grade and were purchased from Merck, UK. The pH of the feed solution was reduced from 7.1 to 6.3 due to the reverse solute flux from the draw solution to the feed solution. It might be true that the acidification can improve the solubility of salt but with care of promoting sulfate scaling. The mixing method and composition of the synthetic saline solutions and BW FS are tabulated in Table 1.

1.2 Measurements of membrane porosity, pore radius, and structural parameter (S)

The structural parameter (S) is correlated to the tortuosity (τ), thickness (t_s), and effective porosity (ε) [2]:

$$S = \frac{\tau\, t_s}{\varepsilon} \qquad (1)$$

Where, τ, t_s, and ε are the sub-layer thickness, tortuosity and porosity respectively. The tortuosity is related to the porosity and expressed as [26]:

$$T = \frac{(2-\varepsilon)^2}{\varepsilon} \quad (2)$$

(2)

To determine the porosity, a wet sample having dimensions of 14 cm X 6 cm was measured (m_1, g) and then reweighted after freeze-drying overnight (m_2, g), with the mass difference giving the water content. The densities of water (ρ_w) and polysulfone (PSf) (ρ_p) are 1.00 and 1.24 g/cm^3, respectively. The overall porosity (ε %) of the sample was calculated by this equation [27]:

$$\varepsilon = \frac{(m_1 - \frac{m_2}{\rho_w})}{\frac{m_1 - m_2}{\rho_w} + m_2/\rho_p} \times 100 \quad (3)$$

(3)

pore radius, was measured by filtration velocity method under 1 bar (0.1MPa) pressure. As we know the porosity, the average pore radius was calculated by Guerout–Elford–Ferry equation [28]:

$$r_m = \sqrt{\frac{(2.9-1.75\varepsilon)\times 8\eta l Q}{\varepsilon \times A_m \times \Delta P}} \quad (4)$$

In which η corresponds to the water viscosity of 8.9 x 10^{-4} Pa. s, l is the membrane thickness that measured by using SEM. Q is the volume of water permeate per unit time ($m^3\ s^{-1}$), A_m and P are the effective membrane area (m_2), and the applied pressure of 0.1 MPa (1 bar)respectively.

2.3 Membrane characterization

Scanning electron microscopy (SEM) instrument coupled with energy-dispersive X-ray spectroscopy (EDS) (Hitachi, Japan) were used to characterize the surface and cross-section of the selective and support layers [28]. Prior to SEM imaging, samples were coated with platinum to ensure a conductive surface. Water contact angles of the membranes were measured using a sessile drop technique (Fibro DAT 1100, Sweden) and the captive bubble method was performed. A J-shaped needle was filled with DI water and used to produce an air bubble on the inverted immersed membrane surface in a water bath [29]. The contact angle was measured at five different places on either the selective layer or the support layer. Five measurements were recorded, and the arithmetic mean calculated.

AFM measurements were carried out using a Multimode AFM (Veeco Instruments, USA) with Nanoscope IIIa controller (Bruker, US) using manufacturer supplied software. All measurements were made using tapping mode in air with RTESPA tapping mode probes (Bruker, US). Scan sizes used were 1 x 1 and 5 x 5 μm for all samples.

Membrane surface zeta potentials were calculated from streaming potentials determined using an asymmetric clamping cell connected to an electro-kinetic analyzer (EKA, Austria) [30]. The pH of the test solution 1 mol/L NaCl was adjusted in the range of 3.0 – 9.0 by adding drops of 0.1 mol/L NaOH or 0.1 mol/L HCl. At each pH value, 6 streaming potential measurements were carried out.

1.4 Bench scale forward osmosis set-up and FO filtration experiments

The design of the FO rig is illustrated in Figure 1. The FO rig used in these experiments involves a cell with dimensions of 16.6 cm x 8.6 cm with a membrane effective area of 8.4 cm^2. Two mesh spacers were used to support both sides of the FO membrane. The DS and FS on both sides of the membrane were circulated by two gear pumps. The cross-flow of both solutions was operated in counter current flow, i.e. with anti-parallel flow directions. The cross-flow rate was adjusted to 100 ml/min, which produced a cross-flow velocity of 5.2 cm/s. The initial volumes of both the FS and DSs were 2 liters. The DS reservoir was placed on a weighing scale (Precisa, UK) connected to a computer data logging system. The temperature of both solutions was constant at 20.5°C during all experiments. The conductivity was measured by two calibrated conductivity meters (Jenway Man-Tech 4510,

UK) and HI-8734 Multi-range TDS Meter (HANNA instruments, UK) placed in the FSand DS tanks, respectively.

All FO tests were carried out with a membrane configuration of the selective layer against the FS. The membrane was stabilized using DI water for 20 minutes under the same conditions prior to FO experiments. At the beginning, the baseline experiments of a pristine membrane were determined using DI water FS and 1.0, 1.5, and 2.0 mol/L of NaCl DS. After that, the DI water was replaced by different compositions of synthesized saline solutions. The membrane was cleaned after each test to remove any scaling. Chemical cleaning consisted of HCl solution at pH = 3.0 followed by DI water which were circulated in the FO rig at flow rate of 150 ml/min for 30 minutes. The water flux recovery was determined by measuring the water flux using 1.0 mol/L NaCl as DS and DI as FS under the same conditions. The flux recovery rate was calculated as the percentage ratio of the water flux after cleaning to the initial water flux of pristine membrane [31].

1.5 Determination of water flux, reverse solute flux, Water permeability coefficient (A), and salt permeability coefficient (B) in FO system

Water flux was measured based on the mass change in the draw tank over time. It was produced from the slope of this function:

$$J_w = \frac{(\Delta V)}{A_m \, \Delta t} \tag{8}$$

Where, A_m is the effective membrane area and ΔV (L) is the volume change of the DS over a predetermined time, Δt (h).The concentration of salt flux from the DS to the FS was obtained from a standard conductivity curve plotted using solutions of known concentration. The reverse solute flux (J_s) was determined from [25]:

$$J_s = \frac{C_e \times V_e - C_o \times V_0}{A_m \times \Delta t} \quad (9)$$

Where C_e is the salt concentration in the FS (g L^{-1}) and V_e denoted the final volume of the FS (L) over predominated time Δt (h). C_0 is the initial salt concentration in the FS (g L^{-1}) and V_0 is the initial volume of the FS (L). A_m designated the effective membrane area. To calculate the A and B values from the experimental water flux and salt flux a method by Tiraferri et al. [32] was used. In the FO experiment, a DI water feed solution (CF) and draw solution concentrations (CD) of 0.5, 1.0, 1.5, 2.0 mol/L were used to measure the water flux J_w and salt reverse flux J_s. Four different values of water flux J_w and reverse salt flux J_S were obtained.

2. Result and discussion

2.1 Characteristics of FO thin film composite membrane

3

The support layer exhibited high bulk porosity of about 63% based on equation.3. Fig.2 shows that the support layer is highly porous with large open pores with support layer thickness of 90.0 μm. Due to low thickness, the structural parameter was small at 489.9 μm. The membrane has a typical structure for a polyamide coating active layer fabricated by interfacial polymerization with thickness of less than 1 μm on top of the polysulfone sub-layer [33,34]. This tight membrane has a mean pore size of 33.6 nm calculated from eq.4. The measured root mean squared (RMS) of the roughness was 26.7 and 36 nm for scan sizes of 1.0 x 1.0 and 5.0 x 5.0 μm respectively. The PSf support layer has an average contact angle of about 52.8°, which is more hydrophilic compared to other membranes reported in the literature (PSf RO=95.2°) (see Fig.3 A) [35]. The active layer had a lower average contact angle of about 33.5° (see Fig.3 B). The results indicate that the membrane surface is negatively charged for most of the pH range (see Fig 4.). The isoelectric point of the membrane was measured at pH 3.2.

2.2 Determination of water and solute flux in FDFO system

2.2.1 NaCl as draw solute

Baseline experiments in the FO system were conducted using four different DS concentrations of NaCl (0.5, 1.0, 1.5, and 2.0 mol/L) as DS and DI water as FS. In comparison with the membrane intrinsic parameters by RO process, A value was obtained corresponding 0.47 LMH , however, B value was lower corresponding 0.04 LMH in FO process. This is because no hydraulic pressure was applied during the FO experiments.

As the osmotic pressure is a colligative property, a high DS concentration will produce greater water flux. In this work, increase in the DS concentration lead to increased water flux, due to the higher osmotic pressure. Water flux in the FO system using NaCl of 1.0, 1.5, 2.0 mol/L as a DS and DI water as a FS was 16.8, 21.0, and 24.0 LMH, respectively (see Fig.5 A), with reverse salt flux of 39.0, 58.0, and 71.0 g/m^2.h respectively. The water flux was 12, 10.1, 8.3, and 7.4 LMH using 1 mol/L NaCl as a DS and synthesized BW (5,000 - 10,000 - 15,000 and 20000 mg/L NaCl) as FS. This water flux also increased on increasing the NaCl concentration, corresponding to 13.7, 12.2, 8.6, and 7.6 LMH when 1.5 mol/L of NaCl DS and (5,000 - 10,000 - 15,000and 20,000 mg/L) synthesized BW were used in the FO process (see Fig.5 B). It was also observed that a significant decrease in the water flux with higher draw solution concentration and higher FS concentration has occurred. It could be explained that the higher DS concentration caused a great initial water flux which influenced the dilution of FS. The reverse solute flux was decreased to 34.5, 30.6, 26.1, and 23.0 g/m^2.h under the same conditions. This can be ascribed to an increase in the osmotic pressure difference between the feed and draw sides of the membrane at high DS concentrations [38]. This means that when the DS concentration was increased, the retention of salts was decreased and the adsorption on the membrane surface was incremented. It can could be explained that as higher DS concentration caused a greater osmotic driving force, more salts could be deposited on the membrane surface. This led to a reduction in the reverse salt flux from the DS to the FS. On the other hand, when lower DS concentration produced low osmotic driving force, the salts might be deposited slowly on the membrane surface. This indicated a slow retention propensity of salts and lower reduction in the water flux. In all cases, there was a drastic decline in water flux when increasing feed TDS concentration.

2.2.2 Fertilizer species as draw solutes

Experiments were performed using 1.0, 1.5, 2.0 mol/L concentration of single fertilizer DSs, such as KCl, KNO_3, KH_2PO_4, and a mixture fertilizer DS, such as KCl+ KNO_3 and DI water as a FS to compare the performance of all selected draw solutions. Fig.6 illustrates the variation in water flux for all selected fertilizers DSs, relative to the NaCl DS. Water flux as a function of single and mixed DS concentrations was determined with DS osmotic pressures of 47.3, 44.4, 42.5, 37.59, and 36.9 bar. The ranking of the fertilizer DSs based on the highest water flux was KCl > KNO_3 > KCl + KNO_3> KH_2PO_4, corresponding to 15.0, 12.6, 11.4, and 9.0 LMH, respectively as compared to that for the NaCl DS (16.7 LMH). In parallel, the solute flux was reduced for KNO_3 and KCl accounting for 46.9 g/m^2.h and 36.6 g/m^2.h respectively as compared to that for the NaCl-DS (39.0 g/m^2.h) (see Fig.7).From the above results, it can be summarized that, the water fluxes produced when utilizing DS fertilizers, were lower than the water flux generated when utilizing NaCl draw solutions at equal molar concentrations. This is mainly because of its high solubility and the dissociation into two ions when dissolved in water thereby generating high osmotic dragging force. It is obvious that, the measured water fluxes for the KNO_3 and mixture KCl+KNO_3 were about 30% lower than that for NaCl DS. However, the measured water flux for KH_2PO_4 was even

lower approximately one half of the water fluxes measured for NaCl, which indicates the variation in the osmotic pressure between both the solutions. Possible reasons for this further decrease of the water flux could be due to combined low osmotic dragging force, diffusivity, and the boundary layer of the feed side. This boundary layer may cause an increment of the DS concentration on the FS side of the selective layer and reduces the osmotic dragging force for the penetration of the RSF within the membrane.**2.2.3 nfluence of DS concentration**

Experiments were also carried out using a reference DS (1.0 , 1.5 , 2.0 mol/L NaCl), single NPK fertilizers (KCl, KNO_3, KH_2PO_4), and a mixed fertilizer (KCl $^+$ KNO_3), at various FS (5,000 - 10,000 - 15,000 - 20,000 mg/L NaCl). In comparison with the NaCl DS, water flux of the KCl DS was slightly lower, while it was far behind at the same concentration for single and mixed fertilizer DSs (KNO_3, KH_2PO_4, KCl + KNO_3) when using 1.0 mol/L DS and synthesized BW FS (see Fig.8). More importantly, the membrane showed a similar decrease in the water flux when using higher draw solution concentration due to the dilution of the DS over time, as water is extracted from the FS and transferred to the DS stream and high concentration of the feed. It was found that the increase of water flux was not proportionate to the increase of the DS concentration. The relatively high initial water flux during the earlier part of the test could result in a high diffusion of salts from the DS to the FS. As a result, the effect of ICP was higher than the dilution of the DS because the water flux flows in the opposite direction of solute flux. It was believed that the polarized layers might be remained in the membrane from previous experiments for different concentrations of saline FSs as the cleaning procedure was less effective to remove salt within the support

layer. The scaling impact and cleaning procedure on the water fluxes could be presented based on the flux ratios or water flux recover ratio. It should be noted that, in every test for different draw solution, different membrane is used, while four different feed solutions are used with cleaning of the membrane after each test. A good restore of the initial water flux was achieved at the beginning due to effective chemical cleaning and low initial fouling tendency in/on the membrane surface. This cleaning allowed a high recovery ratio of (79 %) of the initial flux for 1.0 mol/L NaCl DS. Thereafter, the drop in the water flux during the filtration might be due to scaling layers formed by a combination of trapped salts in the support layer and adsorbed salts on the membrane surface. For example, while using 1.0 mol/L KH_2PO_4 DS, the initial flux recovery observed was 53 % and the last was 43 % at high DS concentration (1.5 mol/L). In other words, this cleaning method caused the disintegration of the scaling layer on the selective layer partly or completely which depends on the degree of crystallization on the membrane surface. It is assumed that the lower flux recovery was due to the salts trapped strongly in the support layer which made this cleaning less efficient. Salt trapping could be due to the mesh embedded in the support layer. This mesh may trap the salt in a certain direction causing a random distribution of salt in the support layer. Consequently, more adverse effect of salt deposition in the support layer was observed leading to a decrease in the initial water flux and overall flux recovery. To that end, this cleaning procedure by flushing the membrane surface at higher cross-flow rate could be ineffective against the internal fouling in the support layer. This indicated the drawbacks of increasing the Ds concentration (osmotic driving force) to improve the water permeation. This is because the ICP and ECP can be augmented at high water flux and they can completely offset the high osmotic pressure. Thus, the ICP created

an additional flow resistance of the draw solute through the membrane which lowered the water flux significantly.

2.2.3.2 Reverse solute flux

The reverse solute flux was directly proportional to the concentration difference between the DS and the FS across the selective layer. This can be attributed to the actual salt concentrations across the membrane interface that linked to both the water flux and the solute flux. The results presented in Fig.8 reveals a poor performance of the DS when increasing the salt load in the synthesized BW FS. The increase in feed salinity or high ionic strength diminished the positive effect of the fertilizer DS. It can be seen that almost identical reduction in the water permeation was noted when 1.5, 2.0 mol/L DSs was used at high TDS concentration of 10,000 - 15,000 and 20,000 mg/L in the FS. Figure.9 shows the water flux and RSF dropped remarkably when using highly concentrated DS and synthesized BW feed (5,000 - 10,000 - 15,000 and 20,000 mg/L NaCl) as compared to the baseline tests. From the comparison on the RSF between the reference NaCl DS and KCl, KNO_3, KH_2PO_4, KCl+KNO_3 fertilizer DSs, the KCl single fertilizer DS performed better than other fertilizer. This can be attributed to its good diffusivity and dissociation in water which arises from a low specific weight and high solubility, it showed higher reverse solute flux than other fertilizers DSs.

It can be explained that the anions (Cl^-) have higher mobility in the solution than the cations (K^{+1}). Later, anions with a high diffusion rate attract cations with a lower diffusion rate across

the membrane from the DS to the FS to maintain electroneutrality. Regardless, the lower charge density in KNO_3 DS results in a weak repulsion force on the negatively charged selective layer, causing a poor rejection rate of NO^{-3} and K^{+1} [20]. Such a significant flux reduction is also expected due to the salt accumulation in the feed side arising from the reverse solute flux. Higher DS concentration caused greater accumulation of salt in the feed side. Therefore, a higher amount of salt in the feed side caused elevated osmotic pressure near the membrane surface, resulting in a lower net driving force, and thus, a significant decrease in the water flux. During the experiment, the adsorption of salts anions from the DS side was decreased on the selective layer due electrostatic repulsive force amongst these anions and the negative charged selective layer. In parallel, a repulsive force was also generated between salt ions from the DS and salt ions adhered on the selective layer. This may weaken the osmotic driving force associated with the deposition of salts on the selective layer.

The much lower reverse solute flux of 23.4 $g/m^2.h$ was produced when using 1.0 mol/L KH_2PO_4 DS and DI water FS, which was probably due to its large hydrated radius (see table.3) as compared with other inorganic DSs reported in the literature [36], leading to a reduced diffusion coefficient and thereby affecting its transfer through the support layer. When the species of different components in the draw solution interact, complex species can be formed which influence the degree of dissociation. Low solubility and high specific weight of the DS may induce a decrease in the water permeation [37]. The apparent decrease of reverse solute flux has been documented in an earlier study, when utilizing divalent ions such as Mg^{+2} and SO_4^{-2} as draw solutes [38]. In accordance with earlier studies, our results revealed that the $KCl+KNO_3$ draw solute was transported at a lower velocity due to the presence of minor

divalent ions which hindered the diffusion of the major monovalent ions Cl^- and K^{+1} throughout the membrane. Another explanation is that the electroneutrality of the ions probably reduces the diffusion rate of this mixture DS. As a result, this mixture DS leaked most slowly which could be originated due to low mobility and driving force of the draw solution. It can also be due to a complex interaction of different ions in the DS or between ions and the selective layer such as electrostatic interaction, ion shielding, and steric hindrance [39].

It can be concluded that when solute permeability was high, the solute diffusivity became the main mode of the solution transfer across the membrane. This means that when the DS concentration was high, where the water flux was also high, the RSF contributed significantly to the overall solute flux. On the other side, at lower DS concentration, where the water flux was reduced, the RSF contributed less to the ultimate solute flux. Besides, the loos/compacted structure of the scaling layer on the selective layer and the interaction between different salt ions from the DS and those on the membrane surface could control the RSF into the FS.

2.2.4 Influence of thermodynamic properties

As shown in Table.2, KH_2PO_4 and the mixture KCl+KNO_3 scored the highest viscosity and diffuse at a slow rate within the membrane. It was documented that the phosphate in the KH_2PO_4 DS had the lower diffusivity as compared to nitrate. Subsequently, 1.5, 2.0 mol/L KH_2PO_4 DS is expected to show poor solubility due to a high specific weight, slightly higher density and the highest viscosity, relative to other single DSs. This indicates that the DS with a low molecular weight performs better. Both KH_2PO_4 and KCl+KNO_3 DS exhibited the highest

mass concentration as compared to other DSs. It could be suggested the difference mass concentration probably caused a decrease in the water flux.

Ion charges and hydrated radii may also affect the diffusion rate of the solute through the membrane. For example, NO_3^- has a larger molar volume, leading to a decrease in the ionic charge density, as well as having a smaller hydrated radius and diffuses faster through the membrane than that of the potassium ion, with a larger hydrated radius and slower diffusion (see Table.2). In comparison with NaCl and KCl, they contain monovalent ions that diffuse rapidly through the membrane selective layer. Sodium and chloride ions had the smaller hydrated radius of 0.36 and 33 nm respectively, compared with other inorganic DSs reported in the literature [40]. Phosphate has the largest hydrated radius which is larger than the calculated mean pore size of the membrane surface. Some of these components were rejected and deposited on the membrane leading to fouling. This means the molecular weight, and ion size of the solute is well correlated to the pore size distribution of the membrane surface. Furthermore, the pH of the draw solution could influence the osmotic pressure and the efficiency of the solution. At low pH, there would be a high diffusion rate of the counterions from the draw solution through the membrane to the FS. Hau et al. [36], observed that high pH in the DS produced more charged ions due to the dissociation of charged compounds in the draw solution, thereby increasing the osmotic pressure and improving the water permeation, whilst the RSF of counterions were minimized at high pH.

It must also, however, be mentioned that the accumulation of salt in the porous structure of the membrane may cause pore clogging. This resulted in higher structural parameters which induced the mass transfer resistance of the draw solute within the support layer to the

selective layer. The high porosity in the sub-layer was at the expense of the ICP, which decreased the osmotic force and resulted in lower porosity and poor membrane performance.

2.3 Performance of fertilizers with saline and BW feed solutions

The concentration of the synthetic feed solutions plays a major role in membrane productivity. The BW has a more complex composition than the draw solution and hence, the effect of various FS compositions, namely: individual solution, binary solution, ternary solution, quaternary solution, and BW synthesized solution was evaluated.

When the concentration of the feed solution was changed (5,000 - 10,000 - 15,000 and20,000 mg/L NaCl) while maintaining a fixed DS concentration, the water flux ranged from 9.0 – 6.3 LMH. Fig.10 shows that the water permeation was also reduced when using higher salt load in the feed solution . There was a decrease in the water permeation upon the addition of salt components to the FS. This parallels a more severe reduction in the water permeation observed with 1.0 mol/L DSs (irrespective of the DS type) and higher salt load in the feed solution at various TDS concentrations to water flux with a DI water feed and 1.0 mol/L NaCl DS.

Feed constituents exacerbated the dilutive ECP on the membrane surface, resulting in a sharp water flux decline. The FS contained several types of solutes with different diffusion rates, , and molecular weights that resulted in different degrees of dilutive ECP and scaling. For instance, SO_4^{-2}ions have low hydration energy and lower solubility resulting in a slow diffusion

rate within the membrane. According to the lyotropic series, the forward diffusion of salt containing a sulfate anion can be controlled by the hydrated radii and valence states [41]. Sulfate ions in the FS have a high valence charge with a large hydrated radius and low diffusion rates, relative to monovalent ions (Na^{+1}) and other species in the FS. This causes low mass transfer and rapid precipitation on the membrane surface. It is worth noting that the addition of Ca^{+2} in the FS affects the filtration performance. From Fig.10-E, the water flux showed a noticeable difference when using any of the fertilizers as a DS and synthesized saline solution without Ca^{+2} as a FS. When Ca^{+2} was added into the FS, the water flux was reduced remarkably as compared to the water flux in the baseline test free of the Ca^{+2}. Besides, further reduction in the water flux was observed as higher proportion of Ca^{+2} was injected into the FS. It is generally accepted that Ca^{+2} ions could form a strong chemical bound with the carboxyl group on the selective layer and weaken the decrease the charges of the Ca^{+2} ions. This resulted in high adsorption tendency of the Ca^{+2} ions on the selective layer. Thus, the salt retention was decreased as higher amount of Ca^{2+} was injected into the FS. This would contribute to high adsorption propensity of the selective layer towards Ca^{2+} ions causing severe scaling.

The structure of the TFC membrane may impact the salt accumulation in the feed side. For example, the surface roughness and ridge structure of the selective layer. This layer has impacted the surface interaction with the scaling constituents and high amount of salt deposited in the ridge structure, with strong adhesion between the surface and these components resulting in a thick scaling layer. Also, the selective layer is negatively charged which would increase the interaction between the functional groups in the surface and positively charged divalent salt ions, yielding a slower diffusion of salt ions. When the

concentration of the cations became high, the surface would have had a high adsorption rate resulting in scaling layer formation. In Figure.11, heterogeneous and crystalline salt scaling was clear on the selective layer. Results presented here agreed with earlier studies describing calcium sulfate formation on TFC membranes [17].

In addition to water permeation, the draw solute permeation in the FS was also detected. Given the detrimental effects of the growth of a scaling layer, it may limit reverse salt flux into the FS, causing elevated osmotic pressure near the membrane surface. Consequently, the net driving force would be decreased leading to a serious drop in the water permeation [42]. It was evident that RSF was alleviated because of scaling on the membrane surface, which reduced nutrient loss from the DS. The RSF showed a decrease from 24.3 to 14.2 $g/m^2.h$ when using KCl DS and synthesized BW feed with various TDS concentrations, whereas the RSF decreased from 27.0 to 12.5 $g/m^2.h$ for KNO_3 DS. This indicated that the membrane reduced the salt flux from the DS stream to the FS stream due to Donnan exclusion effects [8]. The transport of sodium ion within the membrane offsets by the transport of potassium ion from the DS to the FS. Besides, the negative surface charge and permeability selectivity trade- off mechanism caused precipitation of salt ions on the surface.

It can be concluded that dilutive ECP is induced by the composition and properties of the FS. It should be noted that the mesh on the feed side might exacerbate scaling or CP, which decreases the surface area for the permeate flux [43]. Although the spacer could improve the turbulence or mass transfer of the solution, the geometric characteristics of the spacer might be affected by the solution transport during FO tests. Besides, the limited wettability of the backing layer may influence the membrane productivity. This polyester

mesh was expected to be less saturated because its wetting was lower than that of the polysulfone sub-layer. When it was dried before water penetrated the mesh, it would be difficult for the mesh to become fully rehydrated which influenced the solution transport across the membrane.

3 Concluding remarks

Brackish water desalination by fertilizer drawn forward osmosis system was investigated in this work. It is concluded that membrane Zeta potential indicated that the negatively charged surface can induce reverse salt flux, leading to scaling on the surface.

Among the selected fertilizers DSs, KH_2PO_4 and $KCl+KNO_3$ were observed to have the lowest water flux using DI water system. Further decrease in the water flux and reverse salt flux were pronounced when using higher concentrations of synthesized BW FS (15,000 and 20,000 mg/L). It was found that when adding $MgCl_2$, Na_2SO_4, KCl, and $CaCl_2$ to the synthesized NaCl feed solution, the water flux decreased gradually due to scaling compared to that obtained in the absence of these salt components. The KH_2PO_4 fertilizer DS contributed significantly to the formation of a scaling layer on the membrane surface due to the RSF.

The main reason for the decrease in the water flux was due to the membrane properties, such as a negatively charged surface, porosity, structural parameter, and feed solution characteristics such as concentration, specific weight and diffusivity of different salt components. These factors caused high deposition of salt constituents on the membrane surface or scaling formation that reduced the water permeation remarkably through the

membrane. It was concluded that NaCl and KCl scored the best performance achieving the highest pure water permeation and moderate reverse solute flux in all experiments. To increase the flux recovery, osmotic backwashing using 1.0 mol/L NaCl solution as FS and DI water as DS, at high cross-flow velocity is recommended for cleaning a scaled membrane. Another option to alleviate scaling or fouling is using anti-scaling or antifouling additives in the DS and/or FS or a pretreatment method to remove TDS from the feed or gas bubbling assisted FO system.. A positively charged nanofiltration membrane could be a more effective option for minimizing scaling and further investigation is recommended. To maximize the performance of this system, there are two ways. To couple FO desalination plant with a membrane distillation system. The latter can be coupled to a power plant thereby building a cogeneration desalination-power plant. The hot gasses released from a power plant can be used to heat incoming feed solution for membrane distillation system. Alternatively, a cheap renewable energy source such as solar power or wind energy could be also utilized to produce power for distillation process thereby reducing operation cost.

Acknowledgments

The authors would like to thank Qatar Foundation for Education, Science, and Community Development for funding the PhD student Wafa Ali Suwaileh.

Figure Captions

Figure.1: A schematic diagram of the FO rig set up.

Figure.2: SEM images of Toray membrane showing large pores and cross section of 90 μm.

Figure.3: Contact angle measured by sessile drop technique for: (A) support layer (average = 50°); (B) selective layer (average =37°).

Figure.4: Zeta potential of the TFC FO membrane as a function of various pH values.

Figure.5: (A) The water flux as a function of the NaCl DS concentration (1.0-1.5-2.0 M) and DI water feed solution. (B) Influence of DS concentration on the water flux in FDFO system using 1.0, 1.5, 2.0 mol/L NaCl DS and DI water feed solution.

Figure.6: Variation of the water flux for all the tested DS. The FO test conditions are 1 mol/L concentration of DSs and DI water feed.

Figure.7: Reverse solute flux of all the fertilizers DS and NaCl reference DS.

Figure.8: Performance of fertilizers DS with concentration of (1.0, 1.5, 2.0 mol/L) during FO filtration and with synthesized BW feed of (5000, 10000, 15000, 20000 mg/L NaCl). KH2PO4 had poor solubility at 2 mol/L.

Figure.9: Experimental water flux and reverse solute flux of NaCl, KCl, and KNO3 DSs. The water flux and reverse solute flux were determined from experiments using 1 mol/L NaCl, KCl, and KNO3 DSs and a synthesized BW feed solution of varying TDS concentration (5000, 10000, 15000, 20000 mg/L).

Figure.10: (A) Water flux when using 1 M fertilizer DS and various TDS concentrations of NaCl feed solution. (B) The water flux when using 1 M fertilizer DS and synthesized saline solution-FS ($NaCl+MgCl_2$). (C) Water flux when using 1 M fertilizer DS and synthesized saline solution-FS ($NaCl+MgCl_2 + Na_2SO_4$). (D) Water flux when using 1 M fertilizer DS and synthesized saline solution-FS ($NaCl+MgCl_2+Na_2SO_4+KCl$). (E) Water flux when using 1 M fertilizer DS and synthesized BW feed ($NaCl+MgCl_2+Na_2SO_4+KCl+CaCl_2$).

Figure.11: (A) Scaling layer formed on the membrane surface after an hour of the filtration test using 1.0 M KH2PO4 DS and synthetic BW feed (15,000 TDS). (B) Salt crystals on the membrane surface (C) showing salt inclusions on the selective layer after FO filtration test using 1.0-1.5 M DSs and synthesized brackish water feed. Dotted line highlights salt inclusions.

List of figures

Graphical abstract

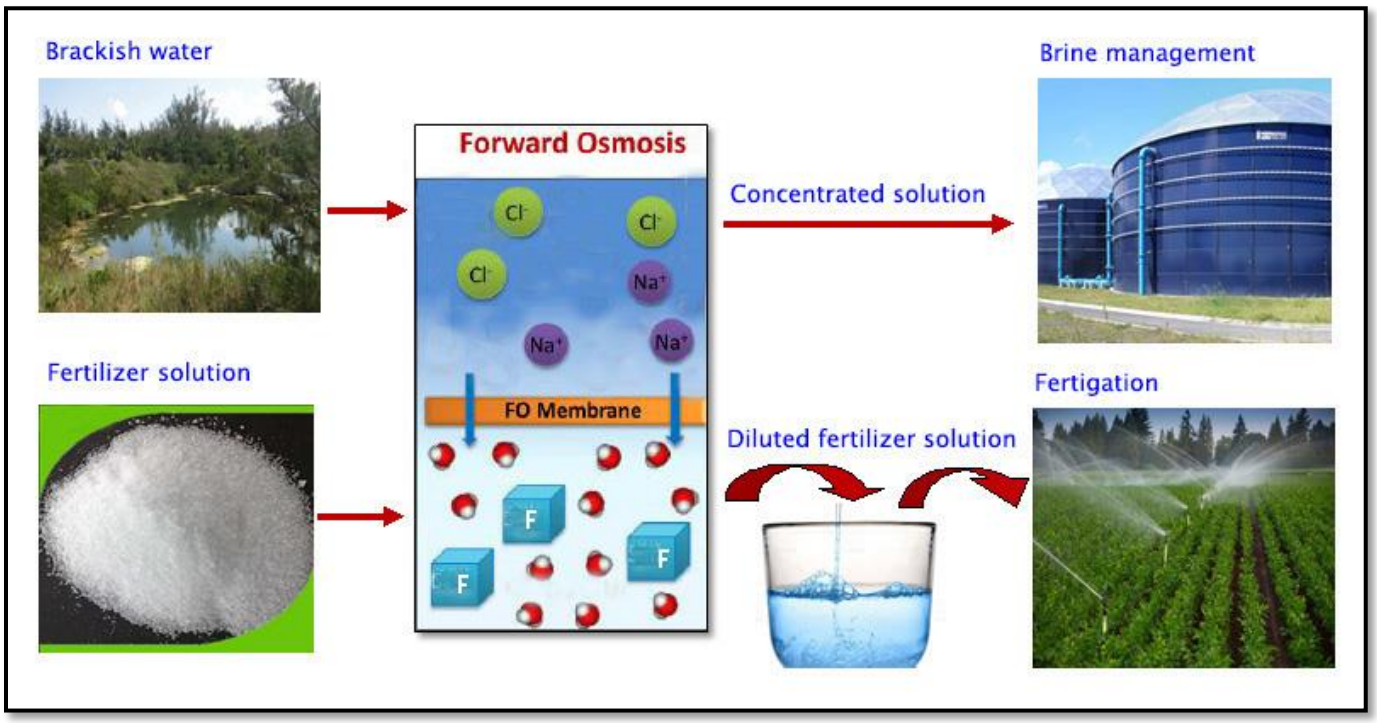

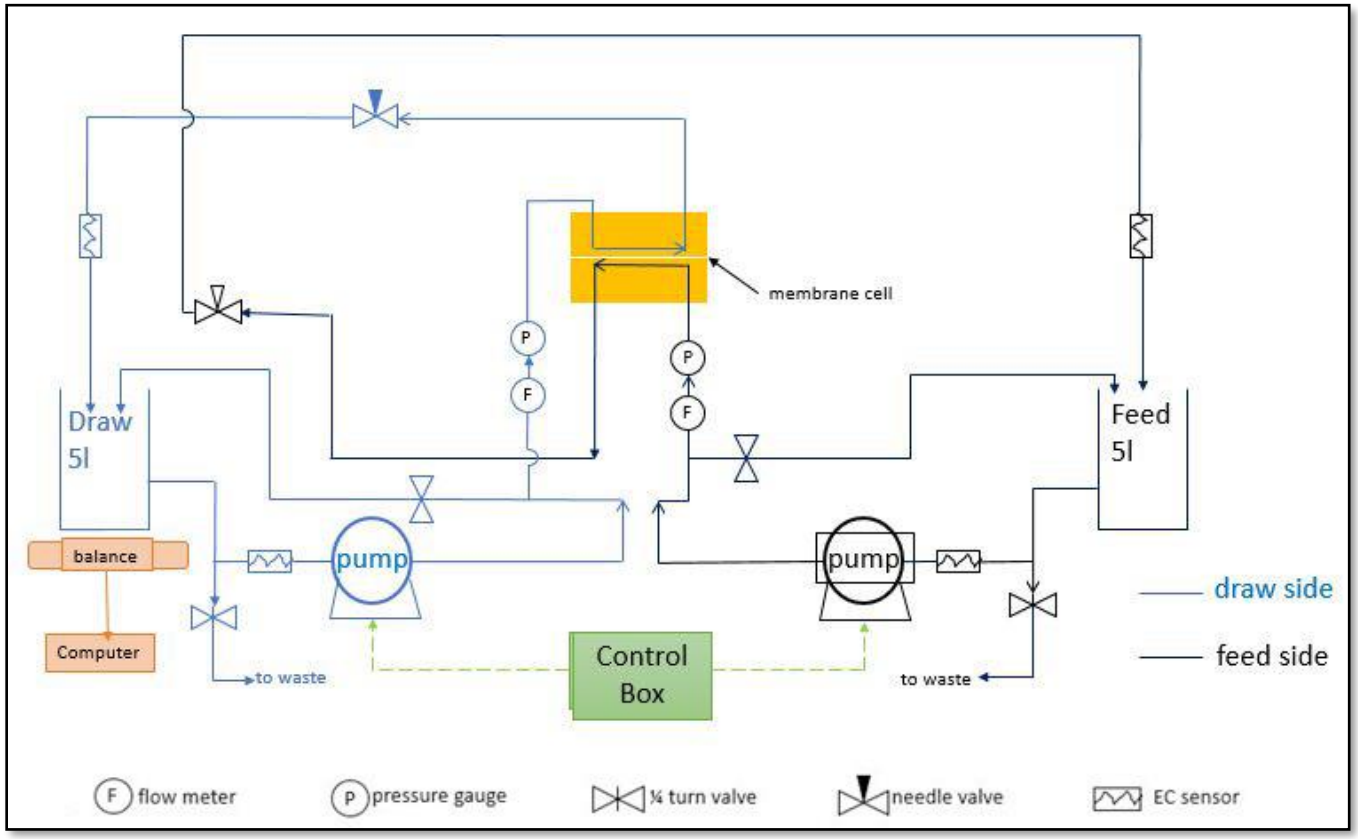
membrane cell
P
F
P
F
Draw
5l
Feed
5l
balance
pump
pump
Computer
to waste
Control
Box
to waste
draw side
feed side
F flow meter
P pressure gauge
¼ turn valve
needle valve
EC sensor

Figure.1

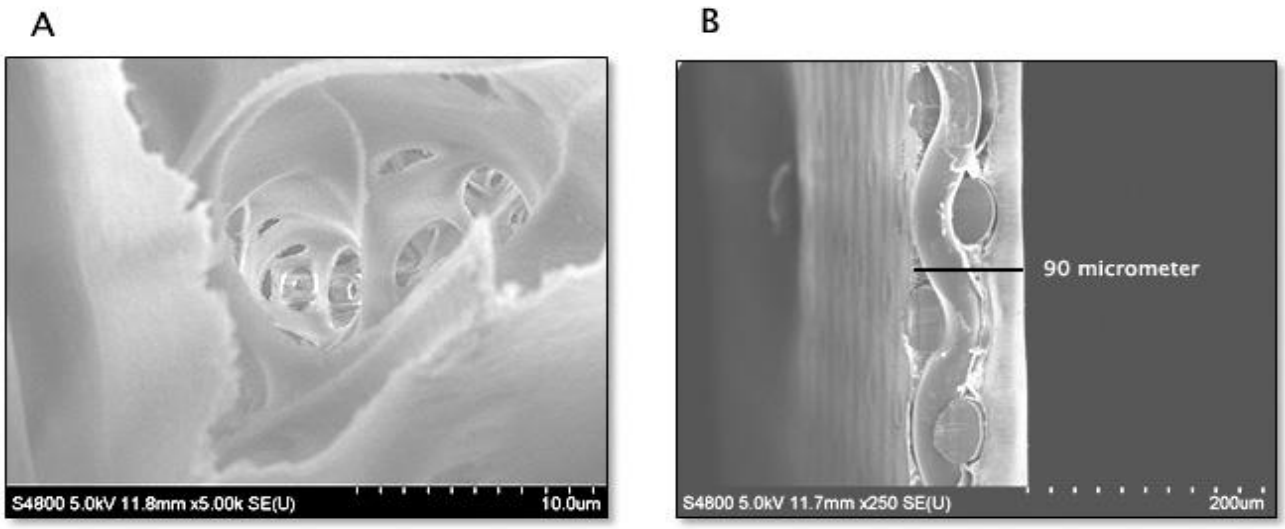

Figure.2

Figure.3

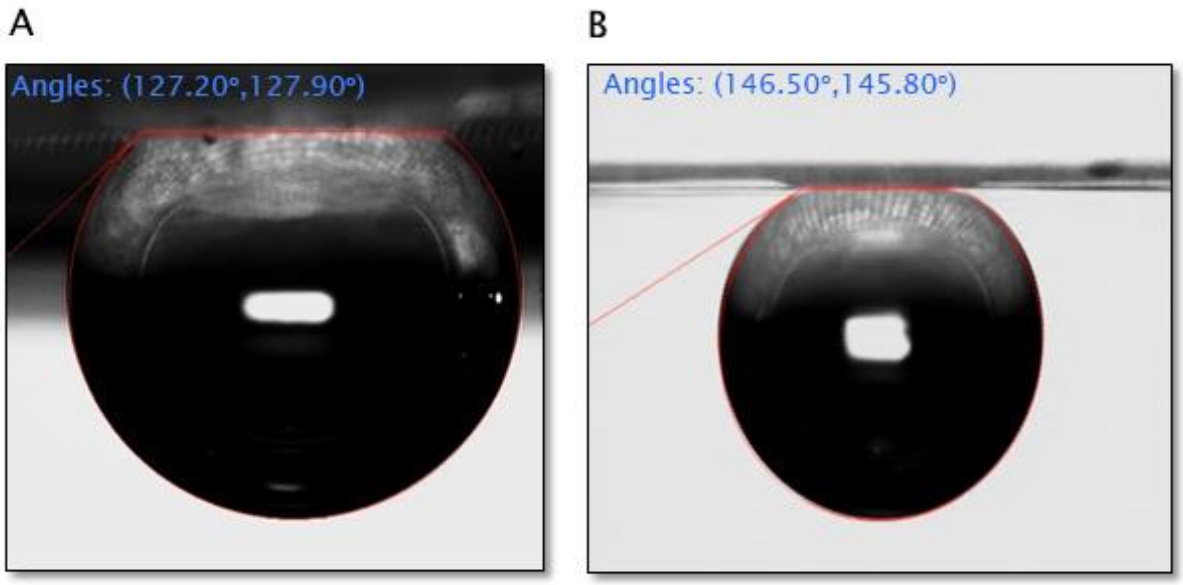

Figure.4

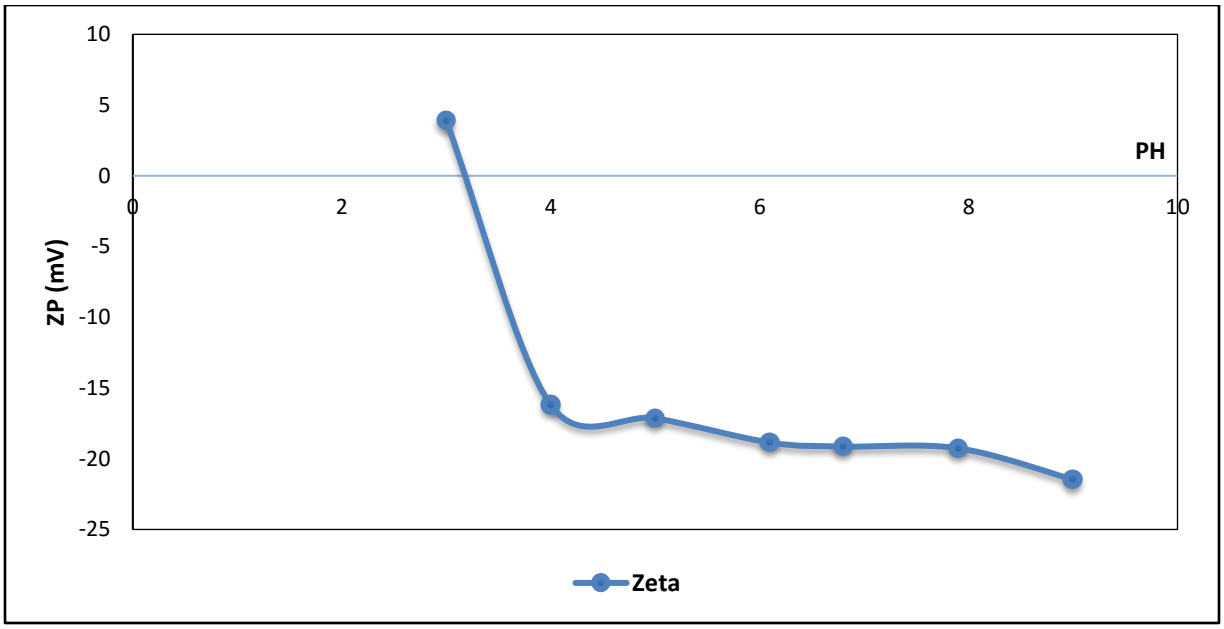
10
5
0
-5
-10
-15
-20
-25
ZP (mV)
0
2
4
6
8
10
PH
Zeta

Figure.5

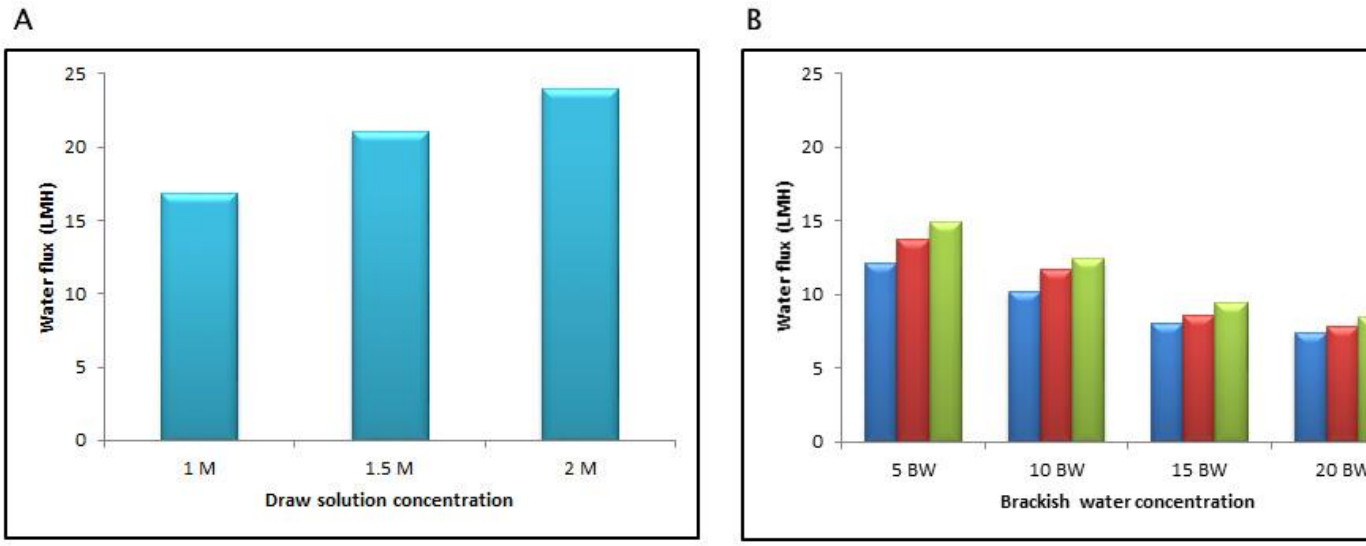
A
25
20
15
10
5
0
Water flux (LMH)
1 M
1.5 M
2 M
Draw solution concentration
B
25
20
15
10
5
0
Water flux (LMH)
5 BW
10 BW
15 BW
20 BW
Brackish water concentration

Figure.6

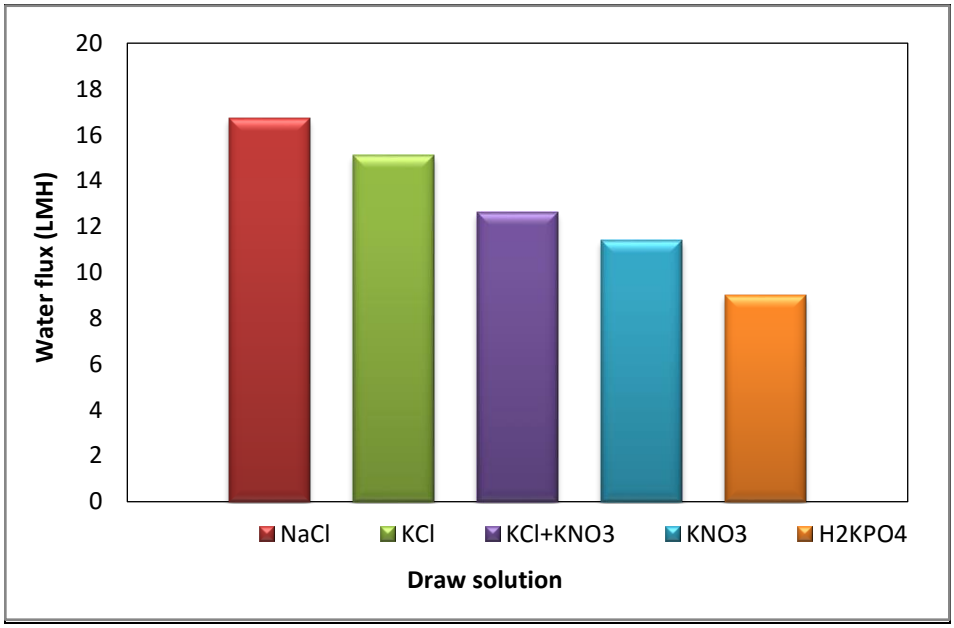

Figure.7

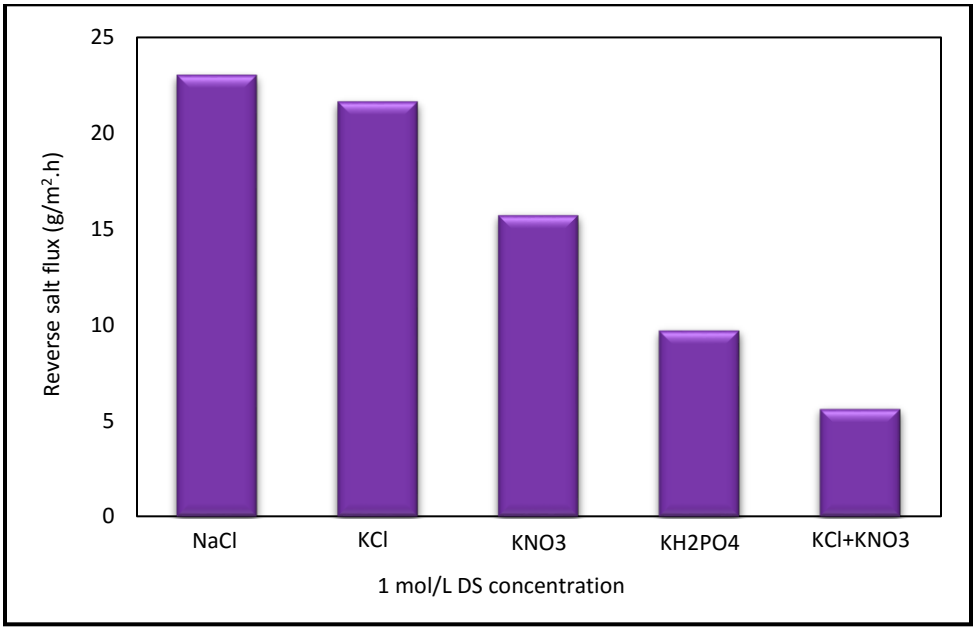

Figure.8

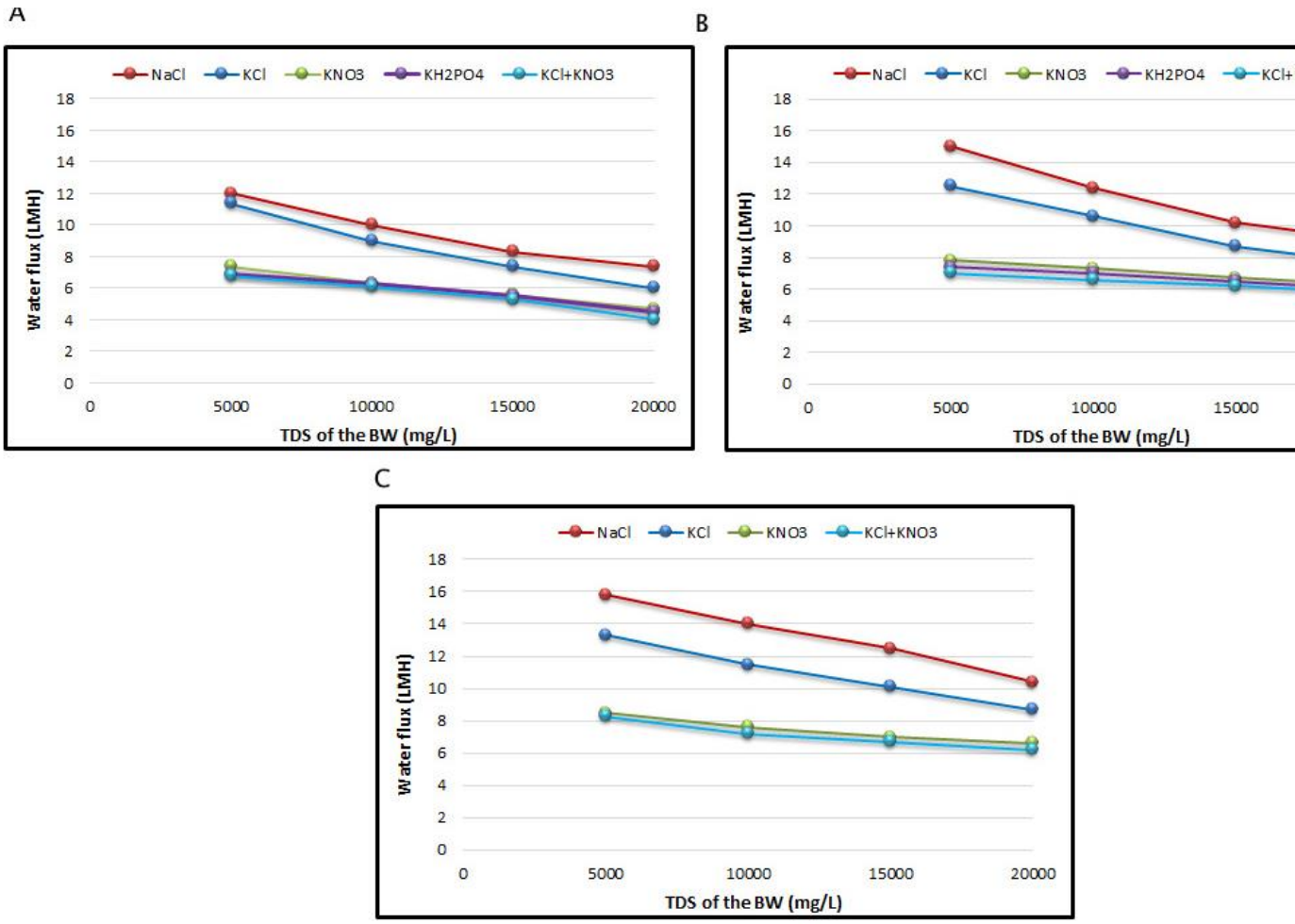

Figure.9

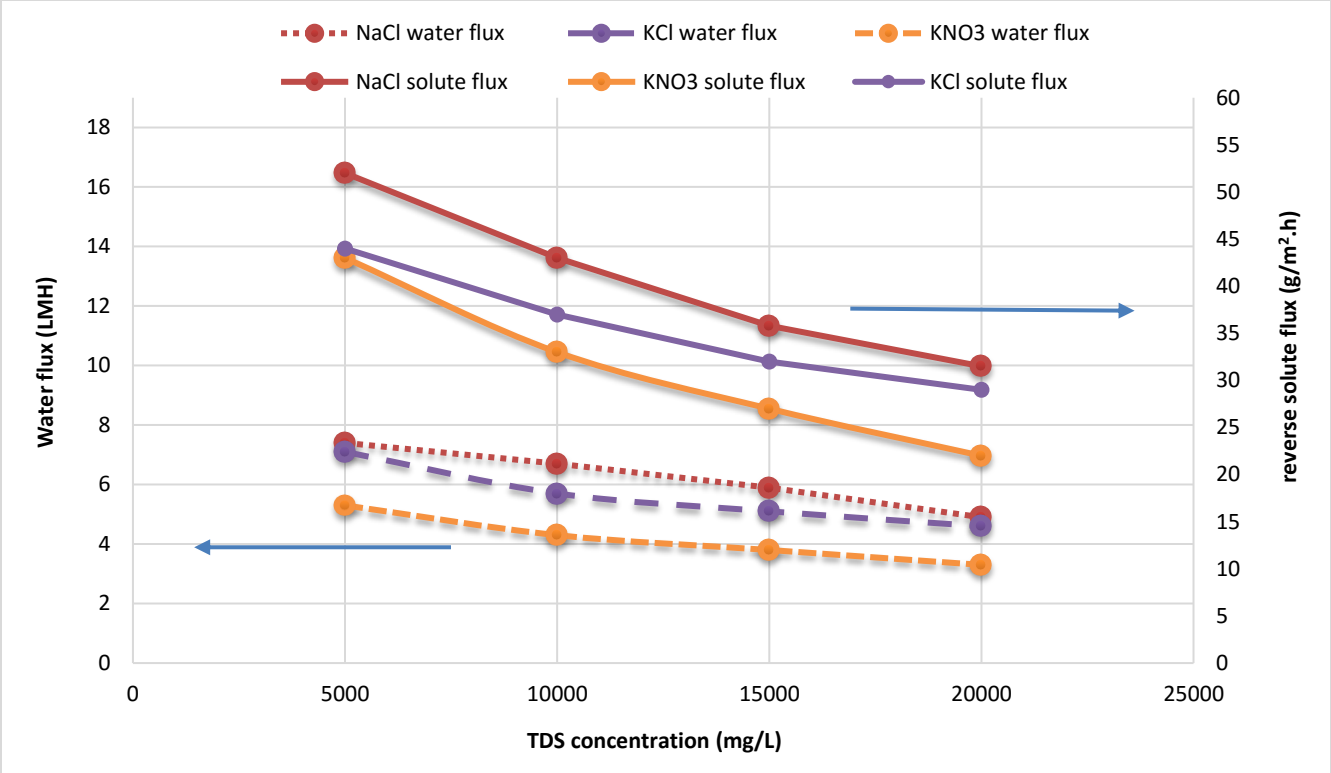
NaCl water flux
KCl water flux
KNO3 water flux
NaCl solute flux
KNO3 solute flux
KCl solute flux
Water flux (LMH)
reverse solute flux (g/m².h)
TDS concentration (mg/L)
0
2
4
6
8
10
12
14
16
18
0
5
10
15
20
25
30
35
40
45
50
55
60
0
5000
10000
15000
20000
25000

Figure.10

A

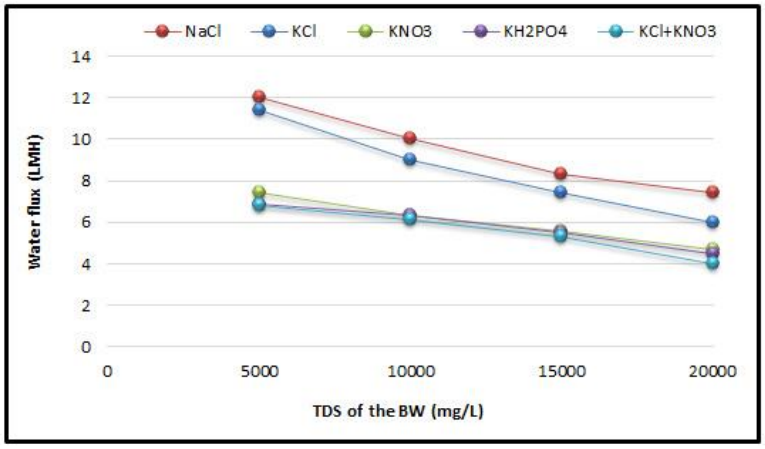
NaCl
KCl
KNO3
KH2PO4
KCl+KNO3
Water flux (LMH)
TDS of the BW (mg/L)
0
2
4
6
8
10
12
14
0
5000
10000
15000
20000

B

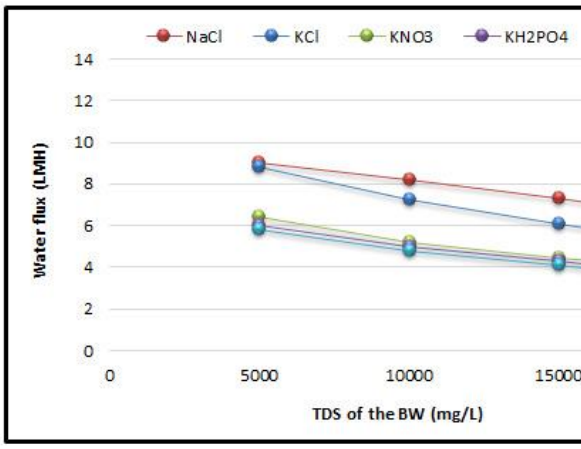
NaCl
KCl
KNO3
KH2PO4
Water flux (LMH)
TDS of the BW (mg/L)
0
2
4
6
8
10
12
14
0
5000
10000
15000

C

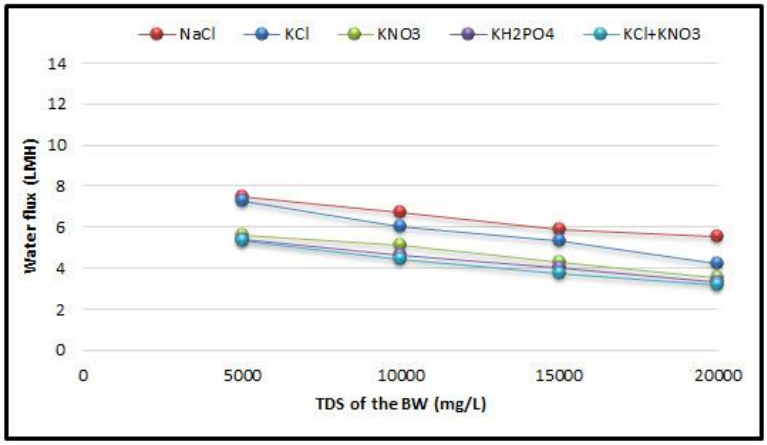
NaCl
KCl
KNO3
KH2PO4
KCl+KNO3
Water flux (LMH)
TDS of the BW (mg/L)
0
2
4
6
8
10
12
14
0
5000
10000
15000
20000

D

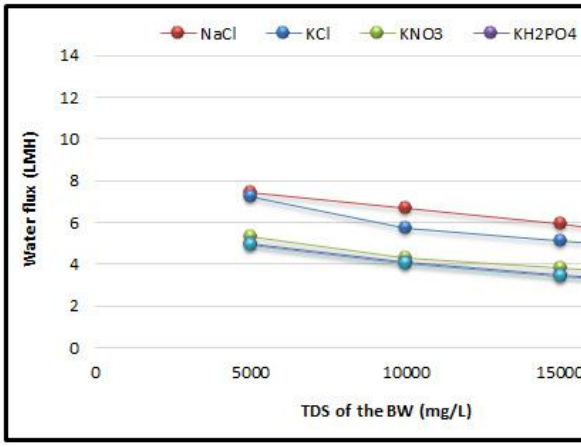
NaCl
KCl
KNO3
KH2PO4
Water flux (LMH)
TDS of the BW (mg/L)
0
2
4
6
8
10
12
14
0
5000
10000
15000

E

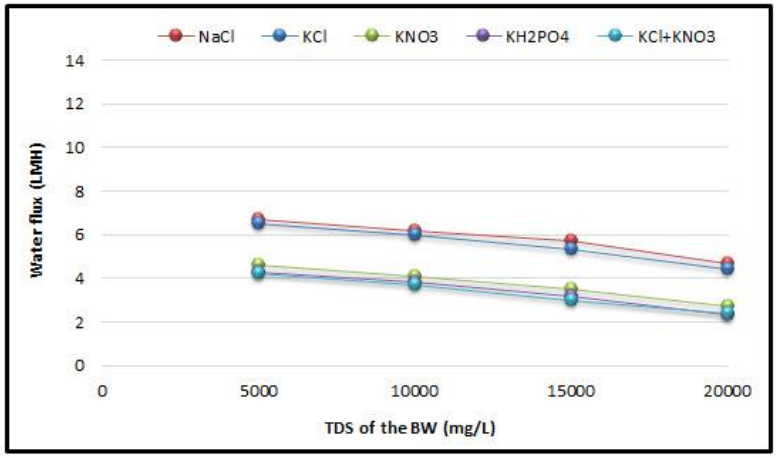
NaCl
KCl
KNO3
KH2PO4
KCl+KNO3
Water flux (LMH)
TDS of the BW (mg/L)
0
2
4
6
8
10
12
14
0
5000
10000
15000
20000

Figure.11

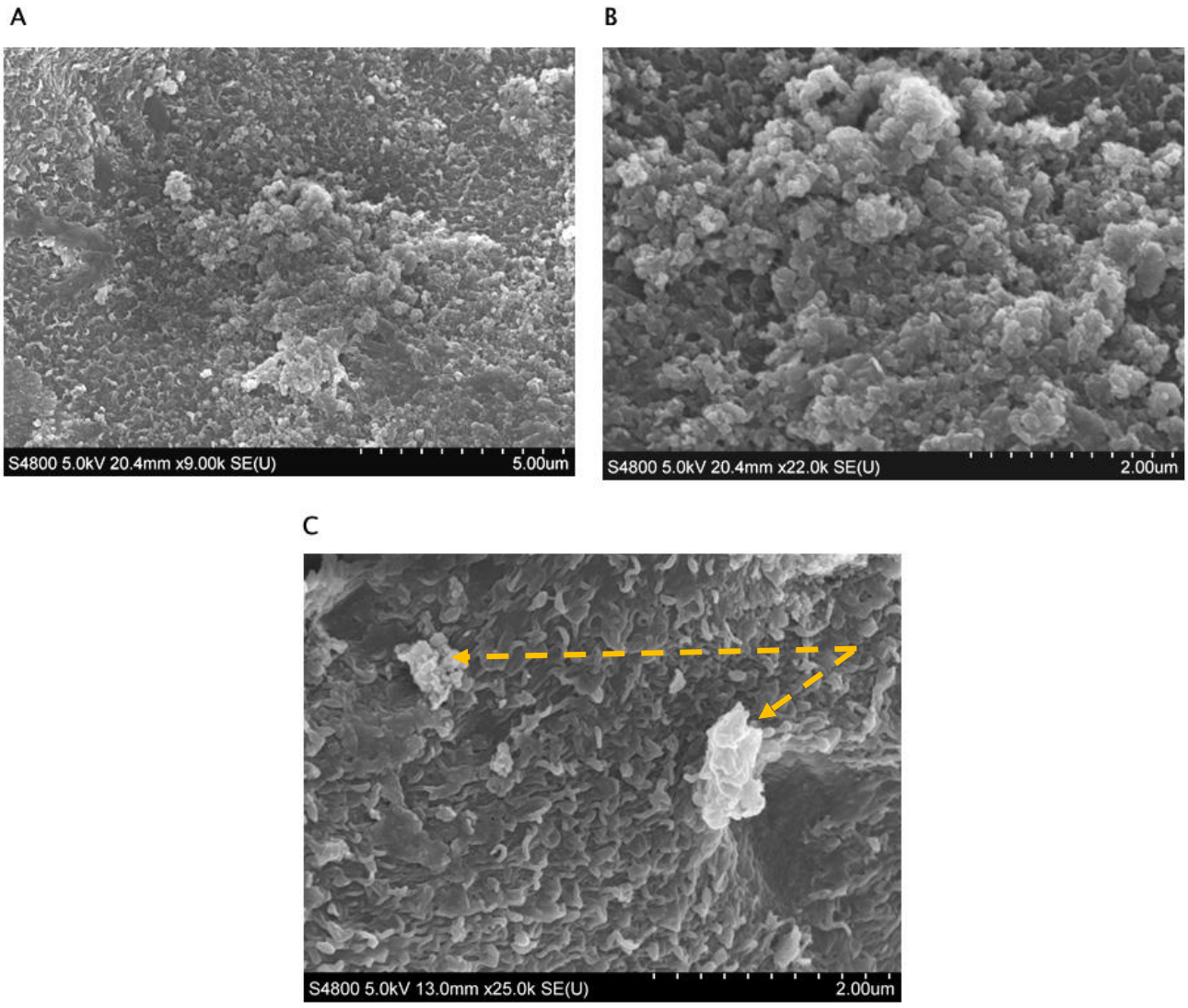

Figure.12

List of tables:

Table.1: Compositions of synthesized saline solutions as a feed with different TDS concentrations used for all FO experiments.

Total (mg/L)	**NaCl (g in 1L water)**	**$MgCl_2$ (g in 1L water)**	**Na_2SO_4 (g in 1L water)**	**KCl (g in 1L water)**	**$CaCl_2$ (g in 1L water)**
5,000	5.0				
10,000	10.0				
15,000	15.0				
20,000	20.0				
5,000	7.25	2.7864			
10,000	14.5	5.578			
15,000	22	8			
20,000	29.04	11.045			

5,000	6.35	2	1.6		
10,000	13.04	4	3		
15,000	19.5	6	4.5		
20,000	26	8	6		
5,000	6.25	2	1.6	0.18	
10,000	12.9	3.9	2.9	0.38	
15,000	19.3	5.8	4.35	0.58	
20,000	25.75	7.75	5.75	0.76	
5,000	3.03	0.7682	0.52227	0.09745	0.15383
10,000	6.06	1.5364	1.0445	0.19491	0.3076
15,000	9.09	2.3046	1.56683	0.29236	0.4615
20,000	12.12	3.0728	2.0891	0.38982	0.6153

Table.2: Thermodynamic properties of different salt components in 1.0 mol/L aqueous solution [37, 40, 44, 45]. Viscosity calculated by OLI analyzer.

Draw solution	**Hydrated radius**	**Diffusion coefficient (m^2/s)**	**Viscosity (CP)**
KNO_3			0.97604
KCl			0.99705
NaCl			1.09298
KH_2PO_4	0.339 nm	-	1.183
$KCl+KNO_3$	-	-	1.973

NO^-_3	0.179 nm	1.900×10^{-9}	-
K^+	0.301 nm	0.44×10^{-9}	-
Na^+	0.36 nm	-	-
Cl^-	0.33 nm	-	-
SO_4^{-2}	-	0.5×10^{-9}	-

References

[1] H. Th. Nguyen, N. C. Nguyen, Sh. Chen, Ch. Li, H. Hsu, Sh. Wu. Innovation in draw solute for practical zero salt reverse in forward osmosis desalination, Ind. Eng. Chem. Res. 54 (2015) 6067 - 6074.

[2] W. A. Suwaileh, D. J. Johnson, S. Sarp, N. Hilal, Advances in forward osmosis membranes: Altering the sub-layer structure via recent fabrication and chemical modification approaches, Desalination 436 (2018) 176–201.

[3] K. Lutchmiah, A. R. D. Verliefde, K. Roest, L. C. Rietveld, E. R. Cornelissen, Forward osmosis for application in wastewater treatment: a review, Water Res. 58 (2014) 179 - 197.

[4] Y. Cui, H. Wang, H. Wang, T. Chung, Micro-morphology and formation of layer-by-layer membranes and their performance in osmotically driven processes, Chemical Engineering Science 101 (2013) 13 - 26.

[5] Q. Yang, K. Y. Wang, T. Chung, A novel dual-layer forward osmosis membrane for protein enrichment and concentration, Separation and Purification Technology 69 (2009) 269 - 274.

[6] Sh. Zou, Y. Gu, D. Xiao, Ch. Y. Tang. The role of physical and chemical parameters on forward osmosis membrane fouling during algae separation, Journal of Membrane Science 366 (2011) 356 -362.

[7] Sh. Zhao, L. Zou, D. Mulcahy, Brackish water desalination by a hybrid forward osmosis–nanofiltration system using divalent draw solute, Desalination 284 (2012) 175 - 181.

[8] H. D. Raval, P. Koradiy, Direct fertigation with brackish water by a forward osmosis system converting domestic reverse osmosis module into forward osmosis membrane element, Desalination and Water Treatment (2015) 1 - 8.

[9] P. Zhong, Fu, X. Chung, T. S. Weber, M. Maletzko, C. Development of thin-film composite forward osmosis hollow fiber membranes using direct sulfonated polyphenylenesulfone (sPPSU) as membrane substrates. Environ. Sci. Technol. 47 (2013) 7430.

[10] A. Giwa, S.W. Hasan, A. Yousuf, S. Chakraborty, D.J. Johnson, N. Hilal, Biomimetic membranes: a critical review of recent progress, Desalination 420 (2017) 403–424.

[11] P. Chen, L. Wan, Z. Xu, Bio-inspired $CaCO_3$ coating for superhydrophilic hybrid membranes with high water permeability, J. Mater. Chem. 22 (2012) 22727.

[12] N. Bui and J. R. McCutcheon, Hydrophilic Nanofibers as new supports for thin film composite membranes for engineered osmosis, Environ. Sci. Technol. 47 (2013) 1761 - 1769.

[13] R. Wang, L. Shi, Ch. Y. Tang, Sh. Chou, Ch. Qiu, A. G. Fane, Characterization of novel forward osmosis hollow fiber membranes, Journal of Membrane Science 355 (2010) 158–167.

[14] W. C. L. Lay, J. Zhang, Ch. Tang, R. Wang, Y. Liu, A. G. Fane, Factors affecting flux performance of forward osmosis systems, Journal of Membrane Science 394– 395 (2012) 151– 168.

[15] Ch. Y. Tang, Q. She, W. C. L. Lay, R. Wang, A. G. Fane, Coupled effects of internal concentration polarization and fouling on flux behavior of forward osmosis membranes during humic acid filtration, Journal of Membrane Science 354 (2010) 123 - 133.

[16] B. Mi, M. Elimelech, Gypsum scaling and cleaning in forward osmosis: Measurements and mechanisms, Environ. Sci. Technol. 44 (2010) 2022 - 2028.

[17] M. Xie, H. K. Shon, S. R. Gray, M. Elimelech, Membrane-based processes for wastewater nutrient recovery: Technology, challenges, and future direction, Water Research 89 (2016) 210-221.

[18] Sh. Phuntsho, H. K. Shon, S. Hong, S. Lee, S. Vigneswarana, A novel low energy fertilizer driven forward osmosis desalination for direct fertigation: Evaluating the performance of fertilizer draw solutions, Journal of Membrane Science 375 (2011) 172 - 181.

[19] D. J. Johnson, W. A. Suwaileha, A. Mohammed, N. Hilal, Osmotic's potential: An overview of draw solutes for forward osmosis Desalination 434 (2018) 100–120.

[20] A. Altaee, G. J. Millar, A. O. Sharif, G. Zaragoza, Forward osmosis process for supply of fertilizer solutions from seawater using a mixture of draw solutions, Desalination and Water Treatment 57 (2016) 28025 - 28041.

[21] M. C. Y. Wong, K. Martinez, G. Z. Ramon, E. M.V. Hoek, Impacts of operating conditions and solution chemistry on osmotic membrane structure and performance, Desalination 287 (2012) 340 - 349.

[22] S. Darvishmanesh, J. Vanneste, E. Tocci, J. C. Jansen, F. Tasselli, J. Degreve, E. Drioli, and B. Van der Bruggen, Physicochemical characterization of solute retention in solvent resistant Nanofiltration: the effect of solute size, polarity, dipole moment, and solubility parameter, J. Phys. Chem. B, 115 (2011) 14507 - 14517.

[23] J. R. McCutcheon, R. L. McGinnis, M. Elimelech, Desalination by ammonia–carbon dioxide forward osmosis: influence of draw and FS concentrations on process performance, J. Membr. Sci. 278 (2006) 114 - 123.

[24] A. Altaee, N. Hilal, High recovery rate NF–FO–RO hybrid system for inland brackish water treatment, Desalination 363 (2015) 19–25.

[25] Z. Wang, J. Tang, Ch. Zhu, Y. Dong, Q. Wang, Z. Wu, Chemical cleaning protocols for thin film composite (TFC) polyamide forward osmosis membranes used for municipal wastewater treatment, Journal of Membrane Science 475 (2015) 184 – 192.

[26] C. A. Scholes, Sh. Shen, Mass transfer correlations for membrane gas-solvent contactors undergoing carbon dioxide desorption, Chinese Journal of Chemical Engineering xxx (2018) xxx–xxx.

[27] S. Sahebi, Sh. Phuntsho, L. Tijing, G. Han, D. S. Han, A. Abdel-Wahab, H. K. Shon, Thin-film composite membrane on a compacted woven backing fabric for pressure assisted osmosis, Desalination 406 (2017) 98 - 108.

[28] Y. Li, Sh. Huang, Sh. Zhoua, A. G. Faned, Y. Zhang, Sh. Zhao, Enhancing water permeability and fouling resistance of polyvinylidene fluoride membranes with carboxylated nanodiamonds, Journal of Membrane Science 556 (2018) 154–163.

[29] Y. Baek, J. Kang, P. Theato, J. Yoon. Measuring hydrophilicity of RO membranes by contact angles via sessile drop and captive bubble method: A comparative study, Desalination 303 (2012) 23–28.

[30] X. Jin, J. Shan, C. Wang, J. Wei, Ch. Y. Tang, Rejection of pharmaceuticals by forward osmosis membranes, Journal of Hazardous Materials 227– 228 (2012) 55– 61.

[31] T. Y. Cath, M. Elimelech, J. R. McCutcheon, R. L. McGinnis, A. Achilli, D. Anastasio, A. R. Brady, A. E. Childress, I. V. Farr, N. T. Hancock, J. Lampi, L. D. Nghiem, M. Xie, N. Yin Yip, Standard methodology for evaluating membrane performance in osmotically driven membrane processes, Desalination 312 (2013) 31–38.

[32] B. Kim, G. Gwak, S. Hong, Analysis of enhancing water flux and reducing reverse solute flux in pressure assisted forward osmosis process, Desalination 421 (2017) 61 - 71.

[33] W. A. Philip, J. Sh. Yong, M. Elimelech, Reverse Draw Solute Permeation in Forward Osmosis: Modeling and Experiments, Environ. Sci. Technol. 2010, 44, 5170–5176.

[34] A. Tiraferri, N. Y. Yip, A. P. Straub, S. R. Castrillon, M. Elimelech, A method for the simultaneous determination of transport and structural parameters of forward osmosis membranes, Journal of Membrane Science 444 (2013) 523–538.

[35] J. R. McCutcheon, M. Elimelech, Influence of membrane support layer hydrophobicity on water flux in osmotically driven membrane processes, Journal of Membrane Science 318 (2008) 458 - 466.

[36] Sh. Phuntsho, S. Hong, M. Elimelech, H. Shon, Osmotic equilibrium in the forward osmosis process: Modelling, experiments and implications for process performance, Journal of Membrane Science 453 (2014) 240 - 252.

[37] N. T. Hau, Sh. Chen, N. C. Nguyen, K. Z. Huang, H. H. Ngo, W. Guo, Exploration of EDTA sodium salt as novel draw solution in forward osmosis process for dewatering of high nutrient sludge, Journal of Membrane Science 455 (2014) 305 - 311.

[38] S. K. Yen, F. M. Haja, N., M. Su, K. Y. Wang, T. Chung, Study of draw solutes using 2-methylimidazole-based compounds in forward osmosis, Journal of Membrane Science 364 (2010) 242–252.

[39] H. T. Nguyen, N. C. Nguyen, Sh. Chen, Ch. Li, H. Hsu, Sh. Wu, Innovation in Draw Solute for Practical Zero Salt Reverse in Forward Osmosis Desalination, Ind. Eng. Chem. Res. 2015, 54, 6067−6074.

[40] Y. Marcus, Thermodynamics of solvation of ions part 5. Gibbs free energy of hydration at 298.15 Kt, J. CHEM. SOC. FARADAY TRANS., 87 (18) (1991) 2995-2999.

[41] N. Hancock and T. Cath, Solute coupled diffusion in osmotically driven membrane processes, Environ. Sci. Technol. 43 (2009) 6769 - 6775.

[42] Ch. Boo, S. Lee, M. Elimelech, Z. Meng, S. Hong, Colloidal fouling in forward osmosis: Role of reverse salt diffusion, Journal of Membrane Science 390 - 391 (2012) 277 - 284.

[43] M. Park, J. H. Kim, Numerical analysis of spacer impacts on forward osmosis membrane process using concentration polarization index, Journal of Membrane Science 427 (2013) 10 – 20.

[44] J. E. Burkell, J. W. T. Spinks, Measurements of self-diffusion in aqueous solutions of sodium dihydrogen phosphate, Canadian Journal of Chemistry 30 (1952) 311-319, https://doi.org/10.1139/v52-042.

[45] D. Krom and Robert A. Berner, The diffusion coefficients of sulfate, ammonium, and phosphate ions in anoxic marine sediments' Michael, Limnol. Oceanogr. 25 (1980) 327-337.